Thin-Walled Structures ▮ (▮▮▮▮) ▮▮▮–▮▮▮

Contents lists available at ScienceDirect

Thin-Walled Structures

journal homepage: www.elsevier.com/locate/tws

Vibration response of an elastically point-supported plate with attached masses

R.J. Watkins *, S. Santillan, J. Radice, O. Barton Jr

Mechanical Engineering Department, United States Naval Academy, Annapolis, MD 21402, USA

ARTICLE INFO

Article history:
Received 8 December 2009
Received in revised form
19 February 2010
Accepted 20 February 2010

Keywords:
Vibration analysis
Modal analysis
Point-supported plates

ABSTRACT

Experimentally determined natural frequencies and modes shapes are presented for an elastically point-supported isotropic plate with attached masses under impulsive loading. These results are compared to frequencies and to modes shapes determined from the Rayleigh–Ritz method and a finite element analysis using COMSOL. Accelerometers mounted at three locations on the plate, provide input for ME'Scope Modal Analysis Software to identify frequency peaks and modes shapes. Orthogonal polynomials, which meet free–free plate boundary conditions, are selected as the basis functions used in the Rayleigh–Ritz method. A Mindlin plate theory, adjusted for negligible transverse shear effects, is used in COMSOL. Frequencies and mode shapes for four plate configurations are presented, compared using each method, and indicate good agreement between the numerical, analytical and experimental results.

Published by Elsevier Ltd.

1. Introduction

Optical beam pointing is quickly becoming a topic of importance and has applications in areas ranging from laser communications to space applications. Potential also exists for development into the next generation of weapon systems. Despite its apparent utility and widespread potential, several factors affect the transmission of the beam from its source to its receiver. Atmospheric effects on beam propagation are important areas of investigation. Turbulence, temperature, and pressure will all affect the beam's coherence and directionality. Structural vibration of the system that houses the optical beam pointing system also dramatically affects its path of motion. If the systems are placed aboard aircraft, mechanical vibrations of the structure are transmitted to the beam. Jitter is the expression coined to describe this induced vibration and describes small amplitude vibration. For example, a 0.01 m diameter optical beam experiencing 1 micro-radian of jitter will result in roughly a nine-fold decrease in the intensity of the beam at distance of 10 km. The United States Naval Academy has developed and built an optical vibration laboratory to investigate the effects of jitter on the accuracy of directed energy beams and to develop control methodologies to reduce its detrimental effect. A key component of this facility is the optical platform.

The optical platform and all of its mechanical elements are modeled as an elastically point-supported plate with attached masses. Point-supported plates are plates that have prescribed displacements at discrete locations within its domain or at specific locations on its edges. Although not typical, displacement derivatives at various locations also can be prescribed. The literature contains a wealth of research which presents the analysis of plates supported on elastic and viscoelastic point supports; only a brief survey is presented here.

Cox and Boxer [1] provided one of the early contributions to this topic and discussed the vibration of a point-supported plate at its corners and free edge boundaries elsewhere. Both rotary inertia and shear effects are neglected for the plate. A finite difference approach is used to solve the governing differential equation providing mode shapes and frequencies for both square and rectangular plates. Amba-Rao [2] studied the vibration of a simply supported rectangular plate carrying a concentrated mass and presents a closed-form solution for the frequencies and mode shapes. To develop the formulae for the frequencies, the transverse displacement is represented as a double infinite sine series. Kerstens [3] incorporates a modal constraint method to solve the problem of vibration of a rectangular, arbitrarily supported plate. The modal constraint approach uses the principle of minimum potential energy which includes virtual work done by homogeneous boundary conditions. Point supports are represented through the virtual work by homogenous boundary condition. A Lagrange multiplier is used to represent the unknown forces. The use of the Rayleigh–Ritz method is a common approach for solving the eigenvalue problem associated with plate vibration. Of particular interest is the selection of basis function used in the analysis. Lee and Lee [4] incorporated a new class of admissible functions to study the vibration of elastically

* Corresponding author. Tel.: +1 410 293 6504; fax: +1 410 293 3041.
E-mail address: rwatkins@usna.edu (R.J. Watkins).

0263-8231/$ - see front matter Published by Elsevier Ltd.
doi:10.1016/j.tws.2010.02.005

Report Documentation Page

Form Approved
OMB No. 0704-0188

1. REPORT DATE	2. REPORT TYPE	3. DATES COVERED
2010		**00-00-2010 to 00-00-2010**

4. TITLE AND SUBTITLE	5a. CONTRACT NUMBER
Vibration Response of an Elastically Point-Supported Plate With Attached Masses	5b. GRANT NUMBER
	5c. PROGRAM ELEMENT NUMBER
6. AUTHOR(S)	5d. PROJECT NUMBER
	5e. TASK NUMBER
	5f. WORK UNIT NUMBER
7. PERFORMING ORGANIZATION NAME(S) AND ADDRESS(ES) **Mechanical Engineering Department,United States Naval Academy,Annapolis,MD,21402**	8. PERFORMING ORGANIZATION REPORT NUMBER
9. SPONSORING/MONITORING AGENCY NAME(S) AND ADDRESS(ES)	10. SPONSOR/MONITOR'S ACRONYM(S)
	11. SPONSOR/MONITOR'S REPORT NUMBER(S)

12. DISTRIBUTION/AVAILABILITY STATEMENT
Approved for public release; distribution unlimited

13. SUPPLEMENTARY NOTES

14. ABSTRACT

15. SUBJECT TERMS

16. SECURITY CLASSIFICATION OF:			17. LIMITATION OF ABSTRACT	18. NUMBER OF PAGES	19a. NAME OF RESPONSIBLE PERSON
a. REPORT	b. ABSTRACT	c. THIS PAGE			
unclassified	**unclassified**	**unclassified**	**Same as Report (SAR)**	**9**	

point supported plates. The basis function corresponds to a similarly supported beam under a point load. Singularity functions are used to completely define the equation of the elastic curve. Normalized frequencies are presented for a plate that is simply supported on all sides, for varying support locations and for several elastic support stiffnesses. Kim and Dickerson [5] incorporate orthonormal polynomials as the basis functions in the Rayleigh–Ritz method to study the vibration of point-supported plates with a combination of simply supported and clamped-edge conditions. The orthronormal set is constructed using the Gramm–Schmidt process. Kocaturk et al [6] considered the dynamic response of a thin orthotropic plate supported on viscoelastic supports. Additional masses are attached to the plate, and the system is subjected to harmonic input. The masses are placed symmetrically along the diagonals of the plate. A Ritz method is used to compute the eigenparameters presented in Lagrange's equations of motion. Results are presented for several material constituents and symmetric modes of vibration consistent with geometry. The authors also present results for the force transmissibility as a function of plate material properties and added mass.

Of particular interest is experimental work that has been done in this area of investigation. Not as voluminous as numerical and analytical work, several contributions are noteworthy in the literature. Nieves et al [7] used laser interferometry to identify the flexural vibrations of a thick isotropic plate. The technique is said to consist solely of out-of-plane displacements and results are compared with those from a Ritz method using a Mindlin plate theory. Lee and Kam [8] considered the effect of elastic-edge supports on the vibration of composite plates as a means of determining the mechanical properties of a plate. Impulse data provided the necessary frequencies to extract the mechanical properties.

Recently, experimental studies of the vibration of an isotropic plate with discrete masses resting on elastic point supports were conducted at the US Naval Academy. Although geometrically similar, measured stiffness of the springs varied by as much as 30%. Several plate configurations were arranged based upon mass placement. The goal of this paper is to compare frequencies and mode shapes extracted from this experimental study with those computed by analytical and computational methods. For completeness, a brief overview of the experimental setup is presented.

2. Experimental setup

The components are mounted on an optical table which is used to isolate effects of external vibrations. The system is used to investigate control methods for mitigating platform vibration and atmospheric effects to directed energy (DE) beams. As part of the investigation, a modal analysis of a rigid aluminum plate mounted on springs and isolators on the optical table was necessary. Fig. 1 shows the elements of the actual mechanical system consisting of the aluminum plate, four mounting springs and vibration isolators, an inertial actuator, accelerometers, and a discrete mass representing a laser source. Several configurations were investigated which varied the location of the mass and actuator mass and are listed in Table 1.

Tables 2 and 3 provide the stiffnesses and masses of various components used in the experimental investigation. Each stainless steel spring is 1.500 in long, with an outer diameter of 1.095 in. The springs are sandwiched between the plate above and air mount below by means of 2 aluminum cups and are not fastened to either the plate or air mount. The spring constants were selected such that the weight of the plate would maintain spring compression during the imposed vibration.

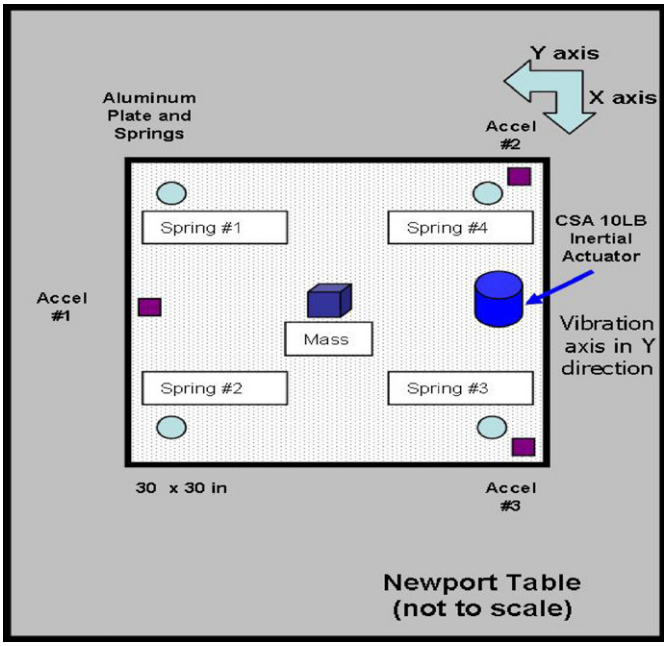

Fig. 1. Plan View of the Experimental Setup.

Table 1
Experimental plate configurations.

Configuration	Description
A	Plate only
B	Plate with mass at center
C	Plate with inertial actuator at center
D	Plate with mass at center and inertial actuator at edge

Table 2
Stiffnesses for spring.

k_{th} Spring	Spring stiffness, lb/ft
1	1517.0
2	1248.2
3	1612.5
4	1401.1

Table 3
Masses for components.

Element	Mass, slugs
Optical platform	1.310
Movable mass	0.118
Inertial actuator	0.185

The plate and spring assembly sit on four SLM-1A air mounts from Newport Corporation. These air mounts are used to dampen the effect of plate motion on the optical table. The mounts were pressurized to 40 psi, resulting in a natural frequency for the air mount of about 3.5 Hz, below the first modal frequency of the plate and spring system of about 5 Hz. The optical table is a Newport RS 4000 series 4 ft by 8 ft by 18 in research grade optical table mounted on 4 Newport I-2000 Pneumatic Isolators with Automatic Leveling. This optical table provides the base support

Please cite this article as: Watkins RJ, et al. Vibration response of an elastically point-supported plate with attached masses. Thin Walled Struct (2010), doi:10.1016/j.tws.2010.02.005

for mounting the components and is pneumatically supported to isolate the table from the environment. The plate is a Newport SA series solid aluminum plate, 30 by 30 by 0.5 in, with drilled and tapped $\frac{1}{4}$ -20 holes on a 1 in grid, with a density of approximately 7 lb/ft^2. The actuator used was manufactured by CSA Engineering Corporation and is capable of providing a variable 10 lb force in a bandwidth of 1–1000 Hz. The actuator is configured to impart multiple frequency periodic motion as well as random vibrations to the plate. The computer control system is based on MATLAB R2006b with SIMULINK from Mathworks, and the xPC Targetbox from SpeedGoat. The main computer for control implementation and experiment supervision is a Dell Precision 690 work station with a CPU speed of 3.8 GHz. The xPC Targetbox is an Intel Core 2 Duo running at 2.13 GHz. Accelerations were measured at three locations using 3-axis accelerometers from Kistler. These accelerometers, model 8690C10, have a resolution of 0.0012 mg_{rms} with a frequency range of 1 Hz–3 kHz, and are driven by a 16 channel Kistler Piezotron Coupler, model 5124A.

3. Analytical formulation

The equation governing the dynamic response of an isotropic plate with added masses resting on spring is given

$$D\nabla^4 w + \sum_{p=1}^{4} k_p \delta(x-x_p)\delta(y-y_p)w(x,y) + \Big(\sum_{q=0}^{N_q} \delta(x-x_q)\delta(y-y_q)m_q + M\Big)w_{,tt} = 0 \quad (1)$$

where D is the flexural stiffness, $w(x, y)$ is the transverse displacement, k_p is the stiffness of the spring located at (x_p, y_p) and m_q is the discrete mass located at (x_q, y_q). Also N_q represents the number of discrete masses on the plate.

For a well-posed problem boundary conditions must be specified. The plate under consideration lies in the $x-y$ plane with the coordinate reference placed at its center so that its edges are located at $x=\pm a/2$ and $y=\pm b/2$. On these edges, the boundary conditions correspond to free edges defined by

$$M_n = 0$$
$$\frac{\partial M_{ns}}{\partial s} + Q_n = 0$$

are prescribed where n represents normal and s represents transverse directions, respectively. The plate is modeled as isotropic and thin with uniform geometry. Four springs, all of varying stiffness, provide support for the plate. Finally, any number of discrete masses can be added to the system. Experimental results are available for two discrete masses providing a framework for a comparison.

Since no exact solution exists for the governing equation, the Rayleigh–Ritz method and COMSOL finite element analysis are used to approximate the natural frequencies and modes shapes.

4. Rayleigh–Ritz analysis

The total potential energy Π for the system containing elastic supports and discrete masses is given as

$$\Pi = U_{plate} + U_{springs} - T_{plate} \quad (2)$$

Here U_{plate} is the strain energy of the plate given by

$$U_{plate} = \frac{D}{2}\iint_R \left\{ \left(\frac{\partial^2 w}{\partial x^2} + \frac{\partial^2 w}{\partial y^2}\right)^2 - 2(1-\upsilon)\left[\frac{\partial^2 w}{\partial x^2}\frac{\partial^2 w}{\partial y^2} - \left(\frac{\partial^2 w}{\partial x \partial y}\right)^2\right]\right\} dxdy \quad (3)$$

where D is the flexural stiffness, ν is Poisson's ratio and $w(x, y)$ is the transverse displacement. The potential energy for the springs is given as

$$U_{spring} = \frac{1}{2}\sum_{p=1}^{4} k_p w^2(x_p, y_p) \quad (4)$$

and the kinetic energy, T_{plate}, is the kinetic energy of the plate and added masses given by

$$T_{plate} = \frac{\rho h \omega^2}{2}\iint_R w^2(x,y)dxdy + \frac{\omega^2}{2}\sum_{q=0}^{N_q} m_q w^2(x_q, y_q) \quad (5)$$

Above k_p is the pth spring stiffnesses and m_q the qth discrete mass. The displacement $w(x, y)$ may be expressed as

$$w(x,y) = \sum_{i=1}^{N}\sum_{j=1}^{N} w_{i_j}\phi_i(x)\theta_j(y) \quad (6)$$

where $\phi_i(x)$ and $\theta_j(y)$ are the shape functions in the x- and y-directions, respectively. In other studies, various types of shape or basis functions have been used including beam shape functions and orthogonal polynomials. Smith et al [9] considered the buckling of isotropic plates under shear loading and solved the corresponding problem using the Rayleigh–Ritz methods. The authors considered a number of orthogonal polynomials as basis functions including Chebyshev type-1 and type-2, Legendre, Hermite, and Laguerre. Here orthonormal polynomials are used as the basis functions which satisfy free–free boundary conditions on all sides and are taken as $\phi_1(x)=1$ and $\phi_2(x)=(x-B_2)\phi_1(x)$. The remaining terms in the sequence are computed from the recursion formula

$$\phi_{k+1}(x) = \{x-B_k\}\phi_k(x) - C_k\phi_{k-1}(x)$$

where $k \geq 2$ and

$$B_k = \frac{\int_a^b x\phi_k^2 dx}{\int_a^b \phi_k^2 dx} \quad C_k = \frac{\int_a^b \phi_k^2 dx}{\int_a^b \phi_{k-1}^2 dx}$$

Also the sequence is normalized satisfying

$$\int_a^b \phi_i(x)\phi_j(x) = \delta_{ij}$$

To arrive at a discrete eigenvalue problem, Eqs. (2)–(6) are combined, and the energy expression is minimized with respect to the displacement coefficients w_{ij}. The resulting equation is in the form

$$\sum_m\sum_n (K_{ijmn} - \omega^2 M_{ijmn})w_{mn} = 0 \quad (7)$$

where the components of K and M are defined by

$$K_{ijmn} = D(A_{im}b_{jn} + \upsilon R^2(C_{im}c_{jn} + C_{mi}c_{nj}) + 2(1-\upsilon)R^2 E_{im}e_{jn} + R^4 B_{im}a_{jn}) + \sum_{p=1}^{4} k_p \varphi_i(x_p)\theta_j(y_p)\varphi_m(x_p)\theta_n(y_p) \quad (8)$$

$$M_{ijmn} = MB_{im}b_{jn} + \sum_{q=0}^{N} m_q \varphi_i(x_q)\theta(y_q)_j\varphi_m(x_q)\theta_n(y_q) \quad (9)$$

In Eq. (8), R is the plate's aspect ratio a/b and M is the total mass of the plate. MATHEMATICA was used for all numerical computations.

Please cite this article as: Watkins RJ, et al. Vibration response of an elastically point-supported plate with attached masses. Thin Walled Struct (2010), doi:10.1016/j.tws.2010.02.005

5. COMSOL finite element analysis

A COMSOL finite element model was developed to compare with analytical and experimental results. This model was built to handle each configuration by placing suitable point masses at the appropriate locations. The model was developed with identical plan-view dimensions, plate thickness and material properties, spring stiffnesses, and spring locations as the above Rayleigh–Ritz analysis.

The model was then meshed with the versatile COMSOL two-dimensional Mindlin plate element from the structural mechanics package. A Mindlin plate model seeks to capture transverse shear deformation effects. However, the above Rayleigh–Ritz model is built upon Kirchhoff plate theory which neglects these higher order effects. To facilitate comparison of the analytical and finite element solutions, the transverse shear factor was reduced effectively to zero in the COMSOL Mindlin plate elements. Structural damping was also neglected.

The mesh had 19 904 elements. The mesh density is dramatically higher in two locations. These two locations correspond to the point mass and/or the actuator mass locations. This single model is suitable for all four configurations considered in this paper, as use of a different mesh is a source of systematic numerical error when comparing results. This mesh density gave sufficient convergence; the numeric values of the resulting natural frequencies are unchanged if a quarter of the number of elements are used.

COMSOL is not a traditional finite element package; it is a numeric partial differential equation solver. This allows for an elegant incorporation of the linear springs by applying displacement proportional forces at the four spring locations. Using the above specified planar mesh and spring loads, a standard COMSOL, undamped, eigenfrequency analysis was performed. Although the software is capable of calculating any number of fundamental frequencies, only the first eight natural frequencies are reported for consistency.

6. Results

Experimental results were compared to both the Rayleigh–Ritz method and the finite element method for each plate configuration. Frequency spectra and frequency response functions were generated by impact analysis. The plate was struck at sixteen locations, and time series were collected from both the impact hammer and the three accelerometers. The accelerometers were located on the plate so that all three could not possibly be located on a nodal line for the first several modes. Fig. 2 presents the frequency response functions (FRFs) for an impact at one corner of the plate. Other FRFs are similar. As shown in Fig. 2, not all frequency peaks appear at every accelerometer location or the peaks have much smaller amplitudes for one or more locations; the modal analysis software (*ME'scope VES, Vibrant Technology, Inc.*) uses this absence or relative magnitude to determine the location and orientation of nodal lines for each vibration mode. Damping ratios are also calculated and are generally on the order of 1%. Frequency response functions and spectra have been generated for configurations B through D.

Finite element analysis provides another means for comparing results and was conducted using COMSOL Multi-Physics modeling software. Both approaches provide frequencies and modes shapes for the four plate configurations shown in Table 1. For the Rayleigh–Ritz method, a convergence study was undertaken to establish the number of terms, N, sufficient for the convergence of the displacement expansion. Results indicate that most modes converge after $N=9$ or N^2 terms in the displacement expansion. For COMSOL, an optimal meshing strategy was incorporated to mesh the solid model of the system resulting in 19 904 elements. (Table 4)

Table 5–7 show frequencies results for each method for the four configurations considered. In each configuration case, the three rigid body modes and the first five bending modes are presented. Table 5 presents experimental results. Configuration A provides a baseline of the mechanical response of an elastically point-supported plate with no added mass. The lowest rigid body frequency of 9.70 Hz corresponds to the transverse mode while

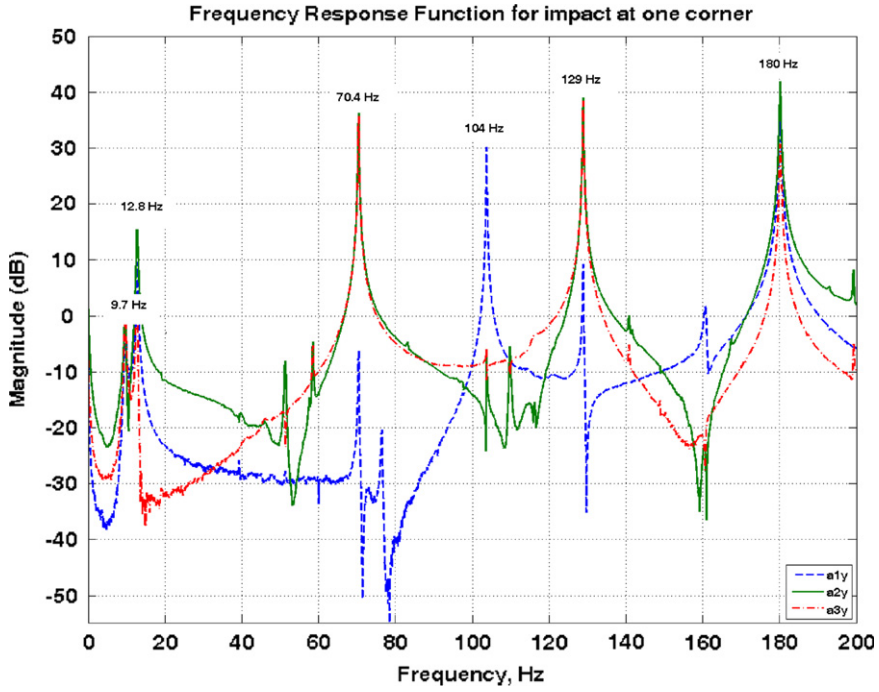

Fig. 2. FRF for Plate Impact.

Please cite this article as: Watkins RJ, et al. Vibration response of an elastically point-supported plate with attached masses. Thin Walled Struct (2010), doi:10.1016/j.tws.2010.02.005

Table 4
Ritz convergence results for the configuration A (Hz).

N	Rigid body modes			Bending modes				
	f_1	f_2	f_3	f_4	f_5	f_6	f_7	f_8
3	9.65	10.4	10.7	77.3	121.2	168.5	225.7	225.7
5	9.64	10.4	10.7	74.4	106.8	134.9	193.2	193.2
7	9.64	10.4	10.7	73.4	106.1	133.4	188.8	188.8
9	9.64	10.4	10.7	73.4	106.1	133.4	188.7	188.7
11	9.64	10.4	10.7	73.4	106.1	133.4	188.6	188.7
13	9.64	10.4	10.7	73.4	106.1	133.4	188.7	188.7
15	9.64	10.4	10.7	73.4	106.1	133.4	188.7	188.7

Table 5
Experimental results for configurations A through D (Hz).

Configuration	Rigid body modes			Bending modes				
	f_1	f_2	f_3	f_4	f_5	f_6	f_7	f_8
A	9.70	12.6	12.8	70.4	104	120	180	181
B	9.30	12.7	12.5	70.5	104	118	180	178
C	9.04	12.7	12.5	72.7	107	121	179	–
D	8.53	11.5	12.6	70.9	96	117	170	181

Table 6
Rayleigh Ritz results for configurations A through D (Hz).

Configuration	Rigid body modes			Bending modes				
	f_1	f_2	f_3	f_4	f_5	f_6	f_7	f_8
A	9.64	10.4	10.7	73.4	106.1	133.4	188.7	188.7
B	9.61	10.1	10.4	73.4	106.1	133.3	188.7	188.7
C	9.40	10.1	10.6	73.4	102.7	131.2	188.8	189.0
D	9.04	9.68	10.4	73.4	102.6	131.0	188.8	189.0

Table 7
COMSOL results for configurations A through D (Hz).

Configuration	Rigid body modes			Bending modes				
	f1	f2	f3	f4	f5	f6	f7	f8
A	10.47	13.41	14.6	74.7	105.9	133.4	187.8	187.8
B	10.02	13.41	14.6	74.3	105.6	120.2	187.3	187.4
C	9.79	13.40	14.6	74.3	105.6	114.2	187.3	187.4
D	9.31	11.94	14.1	74.3	83.12	119.6	163.2	187.3

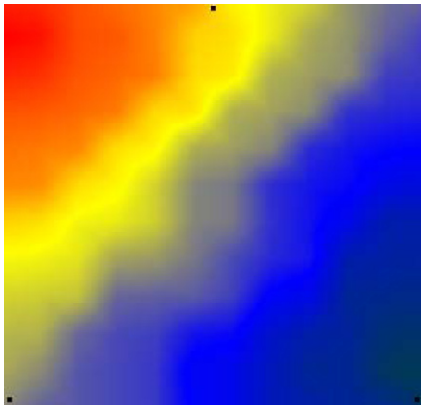

Fig. 3. Rigid Mode 2 Configuration A.

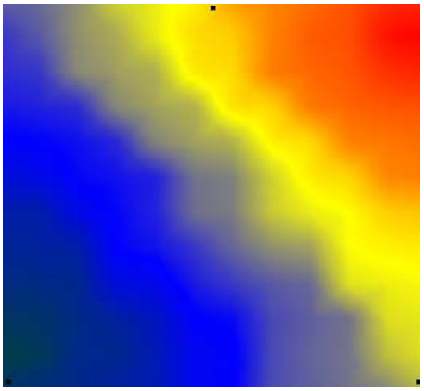

Fig. 4. Rigid Mode 3 Configuration A.

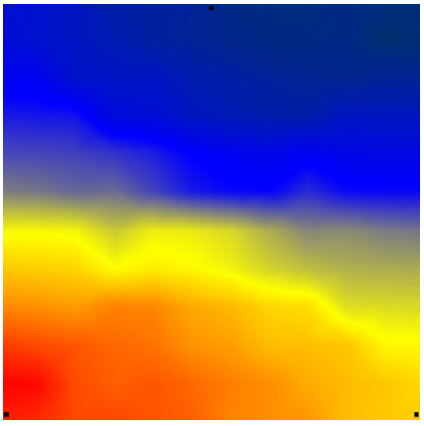

Fig. 5. Rigid Mode 2 Configuration D.

the two frequencies of 12.6 and 12.8 Hz correspond to the rotational rigid body modes, a difference of 2.9 Hz or 31.9% from the transverse mode. Mode shapes for rigid body modes 2 and 3 are presented in Figs. 3 and 4 for this baseline case. Nodal lines are directed along the major diagonals revealing the effect of unequal spring stiffnesses. These nodal lines are orthogonal. Configurations B and C do not differ in their corresponding second and third rigid body mode frequencies, even though there is a significant change in mass added between the two configurations. The effect of added mass can be seen in the first rigid body mode frequency; as expected, the corresponding frequency decreases with increasing mass. But because the masses are placed along nodal lines for the next two modes, the effect of added mass is minimal for these modes.

Configuration D, which includes a centrally located mass and the actuator located on one side, also gives a decreased frequency for the first rigid body mode. This configuration tends to reduce the effect of the unequal spring stiffnesses. The second and third mode shapes for this case are shown in Figs. 5 and 6. Nodal lines are orthogonal to the sides of the plate, similar to those for a plate supported on springs with equal stiffnesses.

Comparing the fundamental frequency from both approaches with the experimental fundamental frequency for configuration A shows that a 0.62% difference occurs with the Rayleigh–Ritz method while 7.94% difference occurs with results computed using COMSOL. For configuration D, the percent differences for this mode are 6.0% for the Rayleigh–Ritz approach and 9.1% for COMSOL. These are the largest of all the cases. Assessing results

Please cite this article as: Watkins RJ, et al. Vibration response of an elastically point-supported plate with attached masses. Thin Walled Struct (2010), doi:10.1016/j.tws.2010.02.005

for configuration C reveals a 20.4% difference exists when compared with the Rayleigh–Ritz for mode 2, while only a 5.51% difference occurs when comparing with COMSOL results. In general, considered modes with larger frequencies result in less accurate frequency comparisons with the Rayleigh–Ritz method, while better agreement is noticed with COMSOL results. The difference in accuracy is most likely due to the orthogonal polynomial basis functions used in the Ritz method.

Figs. 7–11 show modes shapes for the first five bending modes found using ME'scope. The modes are the same for configurations A and D. In these plots, no nodal lines are present, but lines of symmetry are present along the main diagonals in Fig. 8 and along the sides in Fig. 9. Bending mode 3 has no nodes but is symmetric about the plate center. This mode corresponds to the first bending mode of a free–free plate. Modes shapes 4 and 5 are shown in Figs. 10 and 11.

In general, frequencies for a given mode are affected most when the added masses are not mounted along nodal lines. For example, the frequency for bending mode 3 differs significantly for each configuration; the mode has no nodes or nodal lines,

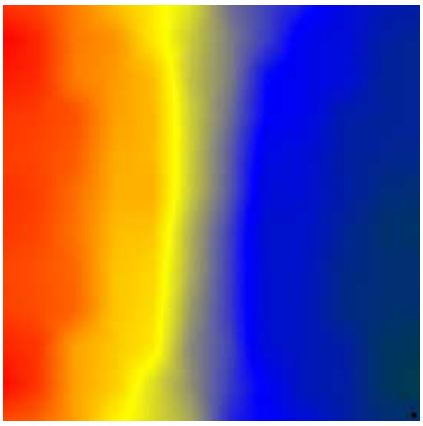

Fig. 6. Rigid Mode 3 Configuration D.

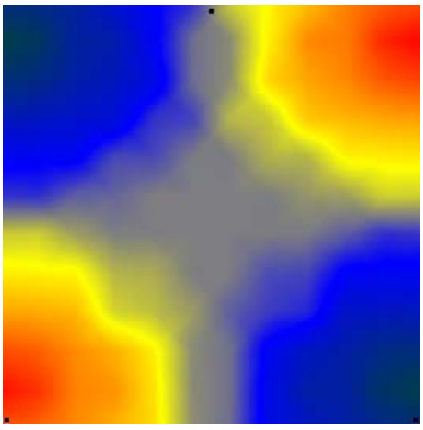

Fig. 7. Bending Mode 1 Configuration A.

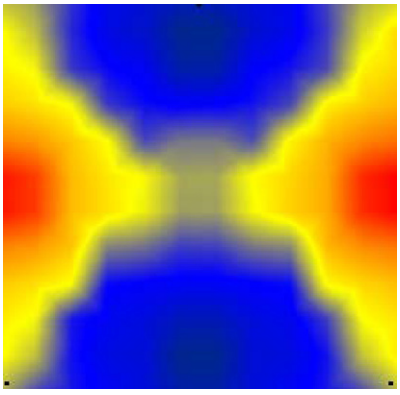

Fig. 8. Bending Mode 2 Configuration A.

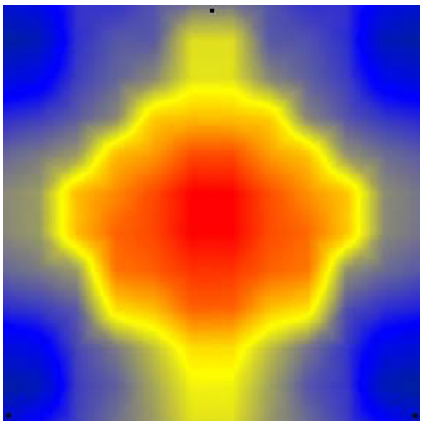

Fig. 9. Bending Mode 3 Configuration A.

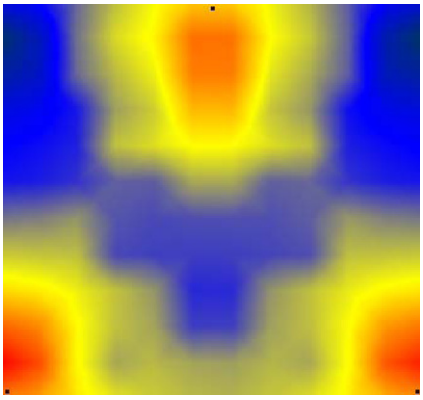

Fig. 10. Bending Mode 4 Configuration A.

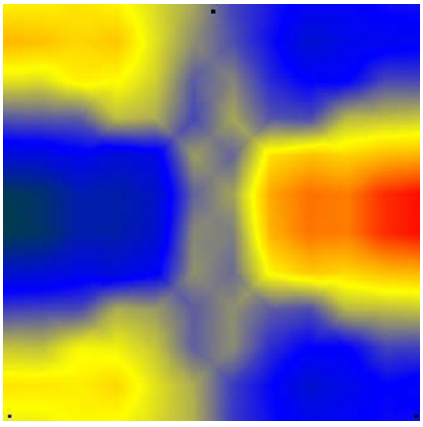

Fig. 11. Bending Mode 5 Configuration A.

Please cite this article as: Watkins RJ, et al. Vibration response of an elastically point-supported plate with attached masses. Thin Walled Struct (2010), doi:10.1016/j.tws.2010.02.005

so no mass could be mounted at a point that would have no effect on the frequency. The frequency for mode 4 differs significantly when configurations A and D are compared. For configuration D, the actuator is placed at a point that does not lie on a nodal line, causing a significant drop in the corresponding frequency. For mode 5, however, the actuator does lie on a nodal line. It can be seen that the frequency for this mode and configuration does not differ from that of configuration A, despite the significant change in total system mass.

Mode shapes for configurations A and D were generated in MATHEMATICA for comparison with experimental mode shapes. Rigid body modes given in Figs. 12–14 are for configuration A, and modes shapes given in Figs. 15–17 are for configuration D. The frequencies of the rotational modes computed by the Rayleigh–Ritz method for configuration A differ by only 0.3 Hz which results in identical rigid body mode shapes for modes 2 and 3. For configuration D, a difference of 0.72 Hz exists between the two rotational modes, resulting in mode shapes that have nodal lines

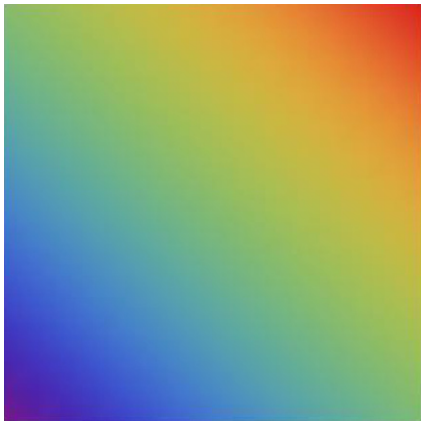

Fig. 12. Rigid Mode 1 Configuration A.

Fig. 15. Rigid Mode 1 Configuration D.

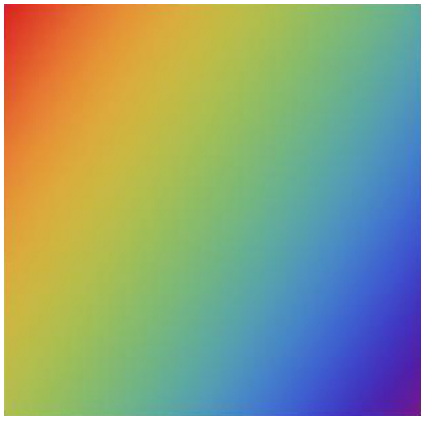

Fig. 13. Rigid Mode 2 Configuration A.

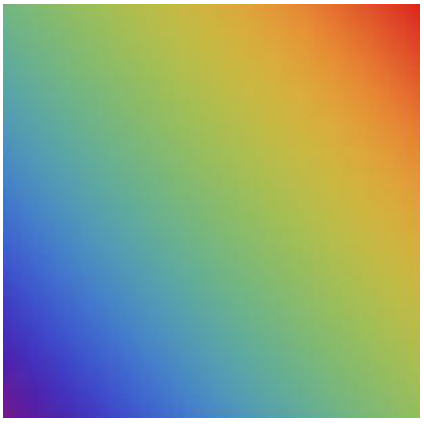

Fig. 16. Rigid Mode 2 Configuration D.

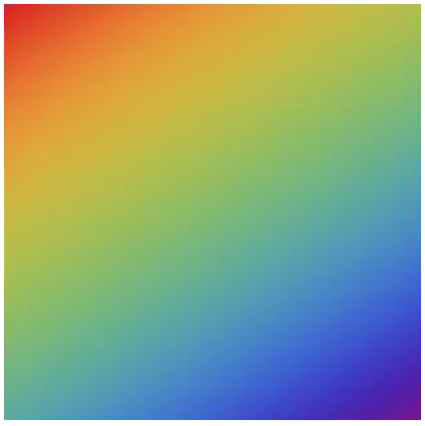

Fig. 14. Rigid Mode 3 Configuration A.

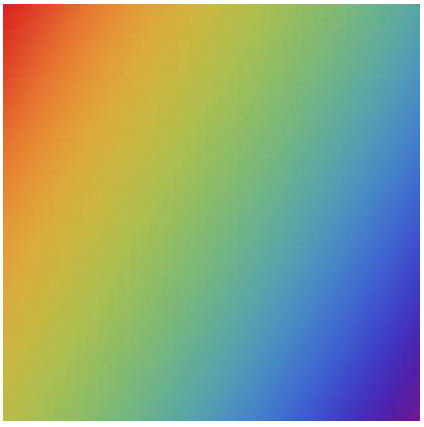

Fig. 17. Rigid Mode 3 Configuration D.

Please cite this article as: Watkins RJ, et al. Vibration response of an elastically point-supported plate with attached masses. Thin Walled Struct (2010), doi:10.1016/j.tws.2010.02.005

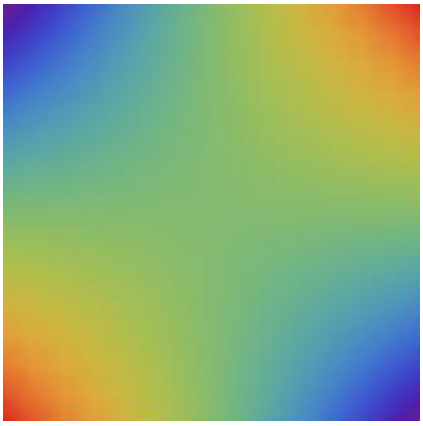

Fig. 18. Bending Mode 1 Configuration A.

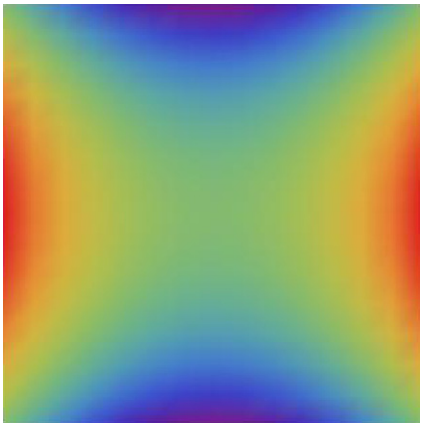

Fig. 19. Bending Mode 2 Configuration A.

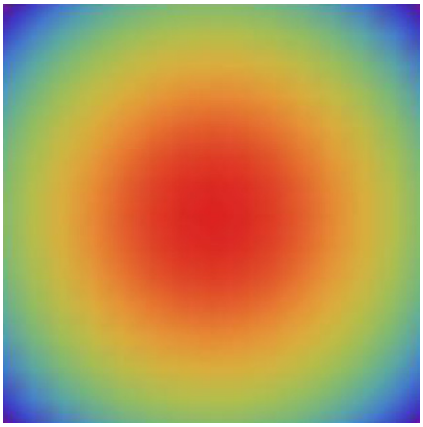

Fig. 20. Bending Mode 3 Configuration A.

that are orthogonal to each other (shown in Figs. 16 and 17). The mode shapes fall short of a favorable comparison with those shown in Figs. 5 and 6.

Figs. 18–22 show the first five bending mode shapes for both configurations A and D. Bending mode shape 3 represents the first bending mode for a free–free plate as extracted from the experimental data. Each mode shape compares favorably with modes extracted by ME'scope software.

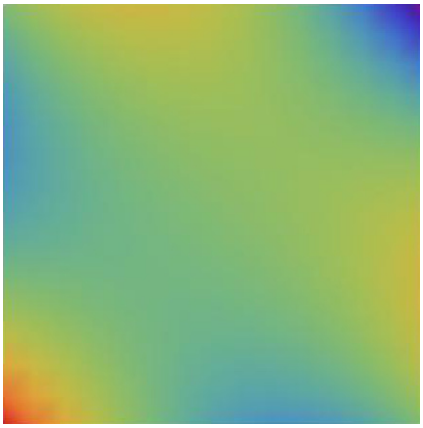

Fig. 21. Bending Mode 4 Configuration A.

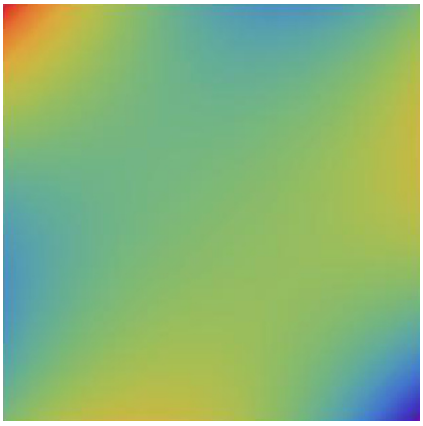

Fig. 22. Bending Mode 5 Configuration A.

7. Conclusion

In the present study, an experimental investigation of vibratory behavior for a spring-supported plate with strategically placed point masses was performed. Using an impact-based measurement method ME'Scope modal analysis software identified the first eight natural frequencies and the corresponding mode shapes. The first three modes were rigid body-type motions of the plate on the springs. The higher frequency modes were more strongly related to bending of the plate. It was observed that the first three rigid body motion natural frequencies were more sensitive to the inclusion of point masses than were the plate bending modes.

These experimental results were subsequently compared to two approximate solutions. The first of the two approximations was the Rayleigh–Ritz-based minimization of the potential energy functional for the idealized spring-mass-plate system from the experiment. The Rayleigh–Ritz analysis invoked orthonormal polynomial shape functions, each of which satisfied the free boundary conditions. The second approximation was a COMSOL finite element model. The COMSOL analysis implemented Mindlin plate elements with transverse shear stiffness suitably increased for comparison with the Kirchhoff plate model of the Rayleigh–Ritz analysis.

The Rayleigh–Ritz analysis was able to suitably capture first three rigid body mode natural frequencies for a majority of experimental configurations. However, there were intriguing differences between the experimentally obtained mode shapes and the Rayleigh–Ritz analysis mode shapes. These results

Please cite this article as: Watkins RJ, et al. Vibration response of an elastically point-supported plate with attached masses. Thin Walled Struct (2010), doi:10.1016/j.tws.2010.02.005

suggest that the selection of basis functions has a significant influence on the accuracy of results obtained from the Ritz analysis. The COMSOL analysis also captured the trend of the rigid body mode natural frequencies, but the predictions were somewhat higher than the predictions of the Rayleigh–Ritz analysis.

Both the Rayleigh–Ritz analysis and COMSOL model were able to effectively capture the experimentally observed high frequency plate bending modes. In general, the two models were in excellent agreement with each other, and slightly higher than the experimental results. These minor differences are to be expected, as both models effectively invoke Kirchhoff-type plate behavior.

References

[1] Cox HL, Boxer J. Vibration of Rectangular Plates Point Supported at the Corners. The Aeronautical Quaterly 1959:41–50.
[2] Amba-Rao CL. On the Vibration of a Rectangular Plate Carrying a Concentrated Mass. Transactions of the ASME, Journal of Applied Mechanics 1964:550–1.
[3] Kersten JGM. Vibration of a rectangular plate supported at an arbitrary number of points. Journal of Sound and Vibration 1979;65(4):493–504.
[4] Lee LT, Lee DC. Free vibration of rectangular plates on elastic point supports with the application of a new type of admissible function. Computer & Structures 1997;2:149–56.
[5] Kim CS, Dickinson SM. The flexural vibration of rectangular plates with point supports. Journal of Sound and Vibration 1987;117(2):249–61.
[6] Kocaturk T, Sezer S, Demir. Determination of the steady state response of viscoelastically point-supported rectangular specially orthotropic plates with added concentrated masses. Journal of Sound and Vibration 2004789–806.
[7] Nieves FJ, Gascon F, Bayon A. Natural frequencies and mode shapes of flexural vibration of plates: laser interferometry detection and solutions by ritz methods. Journal of Sound and Vibration 2004;278:637–55.
[8] Lee CR, Kam TY. Identification of mechanical properties of elastically restrained laminated composite plates using vibration data. Journal of Sound and Vibration 2006;295:999–1061.
[9] Smith ST, Bradford MA, Oehlers DJ. Numerical convergence of simple and orthogonal polynomials for the unilateral plate buckling problem using the Rayleigh–Ritz method. International Journal of Numerical Methods in Engineering 1999;44:1685–707.

Please cite this article as: Watkins RJ, et al. Vibration response of an elastically point-supported plate with attached masses. Thin Walled Struct (2010), doi:10.1016/j.tws.2010.02.005